EFDA–JET–CP(12)06/13

T. Tala, R.M. McDermott, J.E. Rice, A. Salmi, W. Solomon, C. Angioni, C. Gao, C. Giroud, W. Guttenfelder, J. Ferreira, S. Kaye, P. Mantica, Y. Podpaly, F. Ryter, G. Tardini, M. Yoshida, the ASDEX-Upgrade Team, the DIII-D Team, the C-Mod team, the NSTX Team, the ITPA Transport & Confinement Topical Group and JET EFDA contributors

Tokamak Experiments to Study the Parametric Dependences of Momentum Transport

Tokamak Experiments to Study the Parametric Dependences of Momentum Transport

T. Tala[1], R.M. McDermott[2], J.E. Rice[3], A. Salmi[1], W. Solomon[4], C. Angioni[2], C. Gao[3], C. Giroud[5], W. Guttenfelder[4], J. Ferreira[6], S. Kaye[4], P. Mantica[7], Y. Podpaly[3], F. Ryter[2], G. Tardini[2], M. Yoshida[8], the ASDEX-Upgrade Team, the DIII-D Team, the C-Mod team, the NSTX Team, the ITPA Transport & Confinement Topical Group and JET EFDA contributors*

JET-EFDA, Culham Science Centre, OX14 3DB, Abingdon, UK

[1]Association EURATOM-Tekes, VTT, P.O. Box 1000, FIN-02044 VTT, Finland
[2]Max-Planck-Institut für Plasmaphysik, EURATOM-Association, Boltmannstr. 2, 85748 Garching, Germany
[3]MIT Plasma Science and Fusion Center, Cambridge, MA, USA
[4]Princeton Plasma Physics Laboratory, Princeton University, Princeton, New Jersey 08543, USA
[5]EURATOM-CCFE Fusion Association, Culham Science Centre, OX14 3DB, Abingdon, OXON, UK
[6]Associação EURATOM/IST, Instituto de Plasmas e Fusao Nuclear, 1049-001 Lisbon, Portugal
[7]Istituto di Fisica del Plasma CNR-EURATOM, via Cozzi 53, 20125 Milano, Italy
[8]Japan Atomic Energy Agency, Naka, Ibaraki-ken 311-0193, Japan
** See annex of F. Romanelli et al, "Overview of JET Results", (24th IAEA Fusion Energy Conference, San Diego, USA (2012)).*

Preprint of Paper to be submitted for publication in Proceedings of the 24th IAEA Fusion Energy Conference (FEC2012), San Diego, USA 8th October 2012 - 13th October 2012

ABSTRACT.
Several parametric scans have been performed to study momentum transport on JET, AUG, DIII-D, NSTX and C-Mod. NBI modulation technique and RMP coil perturbation have been applied to separating the diffusive and convective momentum transport terms. The magnitude of the inward momentum pinch depends strongly on the inverse density gradient length, with multi-machine experimental scaling for the pinch number being $-Rv_{pinch}/\chi_\phi = 1.1R/L_n + 1.0$. There is no dependence of the pinch number on collisionality whereas the pinch number decreases weakly with increasing q-profile. The Prandtl number was not found to depend either on R/L_n, collisionality or on q. The gyro-kinetic simulations show qualitatively similar dependence of the pinch number on R/L_n, but the dependence is weaker in the simulations. Gyro-kinetic simulations do not find any clear parametric dependence in the Prandtl number, in agreement with experiments. Momentum transport coefficients from each device give quite similar dependences and trends, and therefore extrapolation to ITER seems fairly robust. The extrapolation of these results to ITER illustrates that at large enough $R/L_n > 2$ the pinch number becomes large enough (> 3–4) to make the rotation profile peaked provided that the edge rotation is non-zero. And this rotation peaking can be achieved with small or even with no core torque source.

1. INTRODUCTION

Momentum transport and plasma rotation have been studied extensively on many tokamaks in recent years. Both experiments and theory have shown that sheared plasma rotation can stabilise turbulence while the rotation itself has beneficial effects on MHD modes, such as resistive wall modes. Numerous experimental results have been reported on individual devices – yet no dedicated multi-machine momentum transport experiments have been performed. This paper reports dedicated scans to study momentum transport that have been carried out on JET, DIII-D, AUG, NSTX and C-Mod within the ITPA framework.

2. MULTI-MACHINE TOKAMAK EXPERIMENTS TO EXPLOIT NBI MODULATION (JET, AUG, DIII-D) AND RMP COIL PERTURBATION TECHNIQUES (NSTX) FOR MOMENTUM TRANSPORT STUDIES

NBI modulation technique to create a periodic rotation perturbation has been exploited on JET [1], DIII-D [2] and AUG [3] while on NSTX, 50ms pulses of n = 3 non-resonant magnetic fields were applied, and the resultant relaxation of the rotation after the non-resonant magnetic field was turned off was modelled to extract v_{pinch} and χ_ϕ profiles. More detailed description on that analysis method is reported in Ref. [2]. The NBI modulation experiments have been carried out in different types of plasmas to study the parametric dependencies of momentum pinch and Prandtl numbers. Both in L-mode and H-mode plasmas with NBI modulation, ITGs are the dominant instability on JET, DIII-D and AUG. As the Prandtl number is defined as $P_r = \chi_\phi/\chi_i$, i.e. inversely proportional to the ion heat diffusivity, a comparison of the Prandtl number between different plasmas is more

unambiguous in ITG dominated plasmas where momentum and ion heat transport are tightly coupled. In TEM dominated plasmas or in plasmas where collisional heat transfer between ions and electrons is significant, momentum and ion heat transport are less coupled, thus making $P_r = \chi_\phi/\chi_i$ a less relevant parameter to characterise momentum transport and compare different discharges and parametric dependencies. In most of the NSTX plasmas analysed in this paper, neo-classical transport dominates the ion heat transport channel. Therefore, on NSTX where ITG is not the dominant micro-instability in the heat transport channel (although may still dominate momentum transport), there is no NSTX data plotted in the Prandtl number figures. In fact, a linear stability spectra for one of the NSTX shots used in this study shows the complex spectrum of modes, including overlapping microtearing and ballooning (ITG/TEM/KBM) modes, indicating the complexity of the interpretation of the data. Moreover, the ion scale ballooning modes in NSTX differ from that in AUG, DIIID, JET, in particular the sensitivity to β. Detailed momentum transport studies on these NSTX data with extensive gyro-kinetic analyses are on-going [4].

Typical time traces from a scan to study parametric dependences are shown in figure 1. This is a 3-point collisionality scan performed on JET, which will be discussed in more detail in section 3. In all the AUG, JET and DIII-D experiments, the NBI power and torque were square wave modulated at a frequency $f_{mod} = 6.25$Hz or $f_{mod} = 10$Hz. This frequency is high enough to make the $\mathbf{J}\times\mathbf{B}$ torque the dominant source of torque perturbation everywhere outside $r/a > 0.3$. The modulation cycle is, on the other hand, much longer than the time resolution of the Charge Exchange Recombination Spectroscopy (CXRS) diagnostic used to measuring the toroidal rotation profile ω_ϕ and ion temperature T_i. The modulated power varies from 2–5MW, the power tuned to create an appropriate size of the rotation modulation amplitude of around 5%. Consequently, it is possible to observe changes in toroidal rotation in the beam on and beam off periods and perform the Fourier analysis of the modulated rotation to derive the spatial profiles of amplitude (A) and phase (φ) of the rotation perturbation.

The transport analysis will rely on full momentum transport simulations in which the torque source is assumed to be known precisely enough, with the obvious consequence that any error in the source will cause an error on the derived transport coefficients. It is to be noted here that the NBI torque is the only torque source taken into account in this analysis. Thus the following terms are ignored that could affect the results presented in this paper: residual stress and possible torque sources/sinks due to MHD such as ELMs or NTMs. The analysed plasmas were with type III ELMs and the NTM activity varied from zero to very mild, thus the torque originating from these is negligible as compared with the large NBI torque. The possible role of the residual stress term is discussed later in the manuscript. For the calculation of NBI, the TRANSP code [5] has been used to calculate NBI power and torque profiles as a function of time.

Time-dependent transport modelling of ω_ϕ is required to extract the transport properties from the plasma dynamic response. The transport analysis methodology is in this study to determine the momentum diffusivity and pinch is the same as that described in more detail in [1,6]. It is based

on predictive transport simulations of toroidal rotation using the 1.5D code JETTO and the power and torque sources calculated by TRANSP. The analysis technique is based on minimising the error between the experimental and simulated amplitude, phase and steadystate profiles of the rotation where the transport model for the rotation includes a Prandtl number and a pinch profiles chosen in a way to best reproduce the experimental amplitude, phase and steady-state profiles. As a result, a Prandtl and a pinch profile covering radially the whole radius is obtained (not accurate in the edge region). One of the key features in this multi- tokamak analysis is that AUG, JET and DIII-D data have been analysed with exactly the same tools and analysis method, removing the possibility of uncertainties in the analysis results often arising from different tools when dealing with multi-tokamak data.

3. DIMENSIONLESS COLLISIONALITY SCAN AND THE DEPENDENCE OF MOMENTUM TRANSPORT COEFFICIENTS ON COLLISIONALITY

The standard method to carry out the dimensionless similarity experiment to scan the collisionality, presented in reference [7], has been exploited in this experiment. The main idea is to vary collisionality while keeping the other dimensionless quantities, such as ρ^*, β_N, q and T_i/T_e, as constant as possible. The time traces of the most relevant quantities were already shown in figure 1 from the JET part of the experiment. Within the 3-point scan, collisionality changes over almost a factor of 4. The volume averaged ρ^* and β_N are changing within the scan by about 10% and 20%, respectively. The NBI power modulation and the different power levels between the pulses, required to obtain the collisionality variation, are also shown. A clear modulated toroidal rotation ω_ϕ signal is also visible in figure 1. On DIII-D, ρ^*, β_N, q and T_i/T_e were kept similarly constant to JET at around 10% variation level (the absolute values different from JET though), but in the central part ($r/a<0.4$), R/L_n varied between the three DIII-D pulses significantly, therefore making the collisionality scan invalid in that region. Both JET and DIII-D scans were performed in L-mode because the collisionality scan, while simultaneously keeping R/L_n constant, is not viable to carry out in H-mode plasmas due to the density peaking dependence on collisionality [8]. From the core transport point of view Lmode does not matter as according to GS2 [9] linear gyro-kinetic simulations, these NBI heated low density L-mode plasmas are dominated by the ITG modes.

The averaged momentum pinch number (defined as $-R_0 v_{pinch}/\chi_\phi$) over $0.4 < \rho_{tor} < 0.7$ from the JET and DIII-D dimensionless collisionality scans after the detailed transport analysis are shown in figure 2 (left frame). The momentum pinch number does not depend on collisionality either on JET or on DIII-D. The pinch numbers are higher on JET than on DIII-D, most probably due to R/Ln being of the order 3 on JET and 2 on DIII-D among these pulses. This is an important result, both in view of extrapolating the magnitude of the pinch in ITER and in this study by excluding the effect of collisionality on momentum pinch number in any further analysis of the parametric dependences. Similarly, within this collisionality scan, the Prandtl number does not depend on ρ^*.

On NSTX and AUG, no such a dimensionless collisionality scan was possible to carry out.

However, it is possible to take data from pulses at nearly constant q and R/L_n, and this data has been added into figure 2 (right frame). This confirms further the result from the dedicated JET/DIII-D collisionality scan as no clear trend between the pinch number and ρ^* was found although the variation in ρ^* is very small in AUG shots and the scatter among the points from NSTX is large.

The dependence of the momentum pinch and Prandtl number on collisionality was also studied in linear gyro-kinetic simulations using the GS2 code. The GS2 runs have been performed using the actual data from each shot. The GS2 calculations were performed on a spectrum 6 modes ranging from 0.15 to 0.8, with log spacing, and a spectral shape along reference [10] was used. This choice gives the usual peaking around $k_y\rho_i = 0.25$. In JET, the simulations are fully consistent with the experimental results; neither momentum pinch nor the Prandtl number depends on collisionality. This is illustrated clearly in figure 3 (left frames). In DIII-D (right frames), the simulations tend to weakly suggest that both the Prandt and pinch numbers decrease with increasing collisionality although the dependence is weak. However, in the inner part ($r/a<0.5$) the observable dependence is in fact due to smaller R/Ln of the high collisionality shot rather than due to a real collisionality dependence while on the outer half, R/Ln is matched well among the three shots. In general in momentum transport theory, the pinch and Prandtl numbers do not depend on collisionality [11].

4. DEPENDENCE OF MOMENTUM PINCH AND PRANDTL NUMBER ON INVERSE DENSITY GRADIENT LENGTH R/LN

There is no simple way to perform a clean R/L_n scan in a tokamak without changing some other dimensionless parameter simultaneously. In particular, the strong coupling between the collisionality and R/L_n in H-mode plasmas makes the R/L_n scan without changing the collisionality virtually impossible to carry out. However, since no dependence of momentum transport coefficients on collisionality was found in the collisionality scan experiment discussed in the previous section, it is possible to scan R/L_n by varying collisionality and assign the possible changes in momentum transport to be caused by R/L_n rather than collisionality.

The dependence of the Prandtl number on R/L_n is illustrated in figure 4. The single value of Pr attached to each shot is based on the average value of Pr between $0.4 < \rho < 0.8$. Also, R/L_n reflects the average value from the same radial range. The large range in R/L_n among the shots has been achieved mainly by varying collisionality, density and the amount of the NBI heating power. The variations in q and heating scheme have been kept to a minimum. It is evident in figure 4 that the Prandtl number does not depend on R/L_n as the scatter of the points and the three tokamaks is rather uniform.

The dependence of the pinch number on R/L_n obtained from JET, DIII-D and AUG NBI modulation shots is illustrated in figure 5 (left frame). The shots are the same as shown in figure 4. The pinch number shows a clear dependence on R/L_n on each device separately and also as a joint database. In the right frame, a set of NSTX pulses with similar values of collisionality and q have been added with the points from the other tokamaks. Linear regression for the pinch number gives

$R_0 v_{pinch}/\chi_\phi \sim 1.2 R/L_n$ both for JET and DIII-D, $R_0 v_{pinch}/\chi_\phi \sim 1.5 R/L_n$ for AUG and $R_0 v_{pinch}/\chi_\phi \sim 0.6 R/L_n$ for NSTX. The combined four tokamak dataset yields – $R_0 v_{pinch}/\chi_\phi = 1.1 R/L_n + 1.0$ for the overall dependence.

The increase in the pinch number with increasing R/L_n is qualitatively consistent with theory and gyro-kinetic simulations [11], but quantitatively the simulations give roughly a factor of 2 weaker dependence than found in the experiments [12]. The difference between the experiment and gyro-kinetic simulations is not fully understood. Preliminary simulations with GKW code including the E×B shearing effect [13] have found that this mechanism produces a residual stress which is, however, too small to explain the difference between the predicted and measured pinch velocities. More extended investigations, considering also other residual stress mechanisms like the profile shearing effect [14,15], are planned for future work.

5. 3-POINT Q-SCANS OF MOMENTUM TRANSPORT IN JET AND AUG

A 3-point q-scan was performed on JET and AUG. The magnetic field was kept at B = 3.0T and 2.5T on JET and AUG, respectively, while the plasma current Ip was varied from 1.5MA to 2.5MA and 0.4MA to 1MA, on JET and AUG, respectively. The result of the scan is presented in figure 5 as a function of q at mid-radius. The variation of R/L_n within this 3-point qscan in figure 7 was about 0.4 in JET and 0.3 on AUG, which should result in a change of less than 0.5 in the pinch number according to figure 4 and the corresponding scaling. Therefore, the observed weak q-dependence of the pinch number (larger than 1 unit in $-Rv_{pinch}/\chi_\phi$ in figure 5) seems larger than the one induced by the difference in R/L_n between the high and low q shots. However, taking into account of the actual error bars as indicated in the plot, no solid conclusion can be drawn about the momentum pinch number dependence on q although the scan suggests a weak dependence. The JET points within the q-scan are significantly higher than the AUG ones due to R/L_n being around 3 on JET versus 1.5 on AUG.

One should also note that while q is scanned here, the magnetic shear s is also varied, and the theory suggests in addition to the q dependence that $-Rv_{pinch}/\chi_\phi$ depends also on s [16]. These two effects are challenging to separate from each other in the experiment. The Prandtl numbers for the same three shots are 1.55, 1.39 and 1.81 for JET and 1.55, 1.5, 0.95 for AUG, respectively in the descending order of q for the shots in figure 5. Therefore, one can conclude that no obvious trend between the Prandtl number and q-profile was found within this scan. This is consistent with theory [16].

DISCUSSION AND CONCLUSIONS

The NBI modulation technique has been exploited on AUG, JET and DIII-D to study parametric dependencies of both the momentum pinch and the Prandtl number. This method is a powerful experimental tool to separate the diffusive and convective components of the momentum flux. Exactly the same tools have been used to obtain the momentum transport coefficients from each

device. RMP coil perturbation technique has been used on NSTX.

A dedicated collisionality scan was performed on DIII-D and JET by keeping the other dimensionless quantities (β_N, ρ^*, q, T_e/T_i) constant. No change in the pinch number was observed when the collisionality was varied by a factor of 5 within the scan. In addition, no dependence of the Prandtl number on collisionality was found. Supplementing this data set with shots from AUG and NSTX at constant R/L_n and q increases the scatter, but still confirms the independence of the pinch number on collisionality. Linear gyro-kinetic simulations using the actual data from the JET and DIII-D shots are in good agreement in the pinch number with respect to collisionality dependence.

Within the R/L_n scan, a strong dependence for the pinch number on the inverse density gradient length was observed on JET, AUG, DIII-D and NSTX, the multiple database giving $-v_{pinch}/\chi_\phi \approx 1.1R/L_n + 1.0$. Also, a statistical approach applied to the JET rotation database yields a similar trend [17]. Within the same R/L_n scan, the Prandtl number was not found to be sensitive to R/L_n in these in the multi-tokamak database. On AUG and JET, the pinch number was found to decrease weakly with increasing q, but this dependence is just within the error bars so that no solid conclusions can be drawn. The Prandtl number did not depend on q.

Based on the results from these multi-tokamak parametric scans, one can conclude that the inward pinch will have a significant impact on the rotation profile in ITER provided that the density profile is at least moderately peaked ($R/L_n \geq 1$) and some rotation source is available at the edge of the plasma. In all these analyses, a possible intrinsic torque component has not been taken into account. For the high power NBI shots, like the JET ones, this component will not affect the results significantly, but for lower power shots, like the DIII-D L-mode shots, this term may be significant. By adding an extra edge torque term (like arising from the residual stress) in the analysis method does not modify the inferred pinch and Prandtl number profiles inside $r/a < 0.8$. However, any intrinsic core torque term would instead modify the momentum transport coefficients. The experimental studies on core and edge intrinsic torque terms are on-going (and some reported in ref. [18]) and the preliminary results indicate that the core torque terms seems relatively small compared with the core NBI torque. Still, further experiments and analyses combining these two sources of information are on-going. In addition, there are more NBI modulation shots to be included from DIII-D and AUG and additional data from C-Mod to finalise the scans and find possible other subdominant dependencies, such as ρ^* or β, in addition to R/L_n. Once these experimental parametric dependencies of the pinch and Prandtl numbers as well as the intrinsic torque component are known, reliable extrapolation to ITER becomes possible.

ACKNOWLEDGEMENTS

Work was supported by the European Communities under the contract of Association between EURATOM and Tekes, was carried out within the framework of the European Fusion Development Agreement and the US DOE under DE-FC02-04ER54698 and DE-AC02-09CH11466. The views and opinions expressed herein do not necessarily reflect those of the European Commission.

REFERENCES

[1]. T. Tala et al., Physical Review Letters **102**, 075001 (2009).

[2]. W.M. Solomon et al., Physics of Plasmas **17**, 056108 (2010).

[3]. R.M. McDermott et al., Plasma Physics and Controlled Fusion **53**, 124013 (2011).

[4]. W. Guttenfelder et al., this conference.

[5]. R.J. Goldston et al., Computational Physics **43**, 61 (1981).

[6]. P. Mantica et al., Physics of Plasmas **17**, 092505 (2010).

[7]. T.C. Luce et al., Plasma Physics and Controlled Fusion **50**, 043001 (2008).

[8]. H. Weisen et al., Nuclear Fusion **45**, L1 (2005).

[9]. M. Kotschenreuther et al., Computational Phys. Communication **88**, 128 (1995).

[10]. C. Bourdelle et al., Physics of Plasmas **14**, 112501 (2007).

[11]. A.G. Peeters et al., Physics of Plasmas **16**, 062311 (2009).

[12]. T. Tala et al., Nuclear Fusion **51**, 123002 (2011).

[13]. F. J. Casson et al., Physics of Plasmas **16**, 092303 (2009).

[14]. R.E. Waltz et al., Physics of Plasmas **18**, 042504 (2011).

[15]. Y. Camenen et al., Nuclear Fusion **51**, 073039 (2011).

[16]. A.G. Peeters et al., Nuclear Fusion **51**, 094027 (2011).

[17]. H. Weisen et al., Nuclear Fusion **52**, 042001 (2012).

[18]. W.M. Solomon et al., Nuclear Fusion **51**, 073010 (2011).

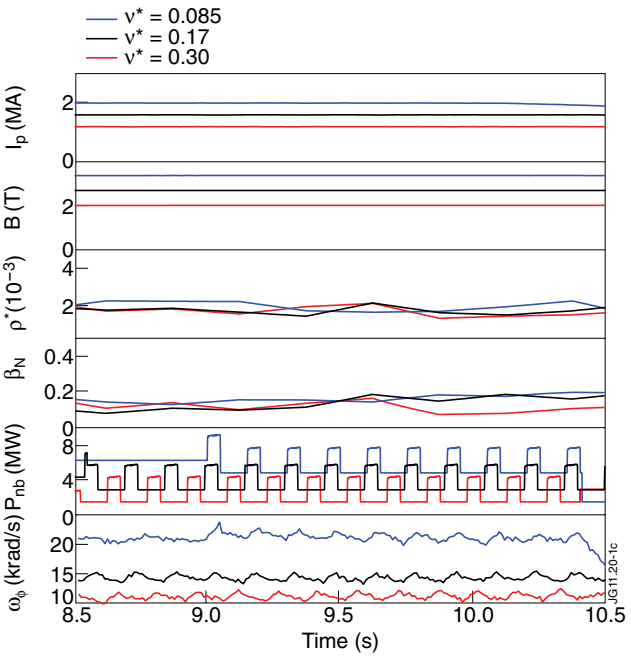

Figure 1: Time traces of plasma current Ip, magnetic field B at magnetic axis, ρ, β_N, NBI power P_{nb} and toroidal angular frequency ω_ϕ at r/a=0.5 for 3 JET Pulses No's. 79811 (blue), 79815 (black) and 79814 (red) with different volume averaged collisionality.*

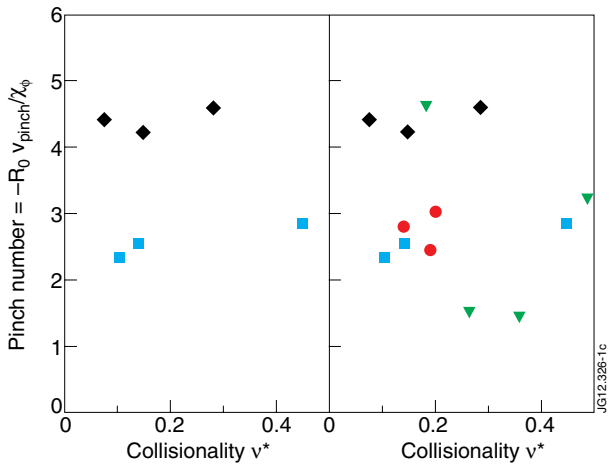

Figure 2: (Left frame) Pinch number as a function of collisionality from the JET (black diamonds) and DIII-D (blue squares) 3-point dimensionless collisionality scans. The data have been averaged between $0.5 < \rho_{tor} < 0.8$. As in left frame, but including data from AUG (red circles) and NSTX (green squares) pulses at almost constant q and R/L_n.

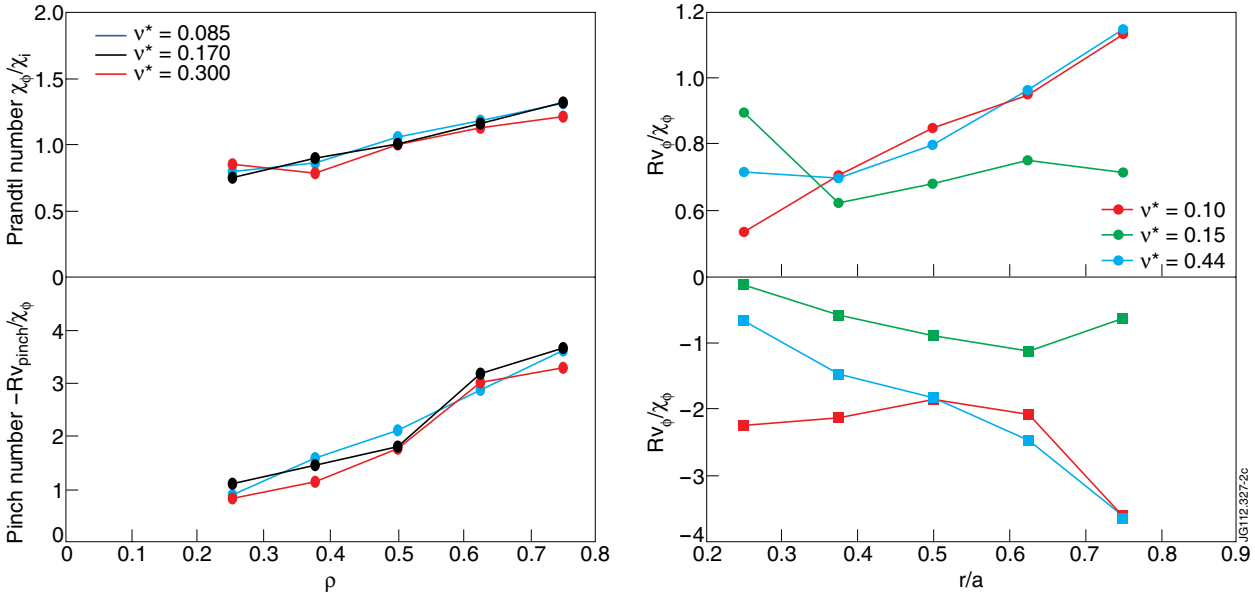

Figure 3: Prandtl number (upper frames) and pinch number (lower frames) profiles for the discharges forming the 3-point collisionality scan as a function of normalised toroidal flux co-ordinate ρ from linear GS2 simulations using the actual input data for JET shots (left) and DIII-D shots (right). The GS2 runs have been performed at five radial locations for each shot.

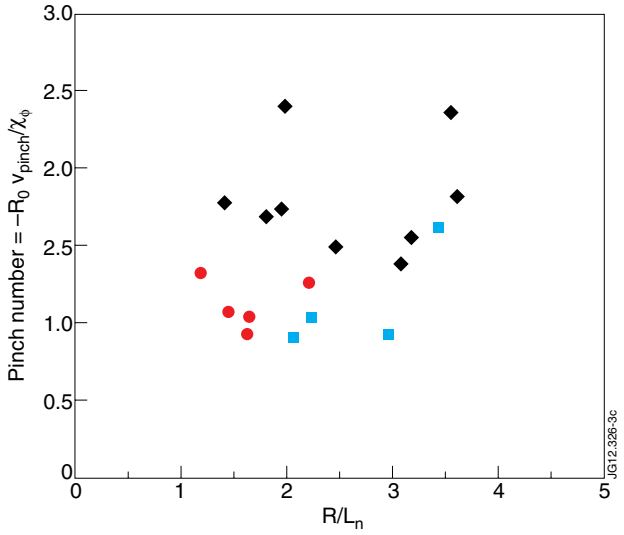

Figure 4: Prandtl numbers averaged over the range 0.4<ρ<0.8, as a function of the inverse density gradient

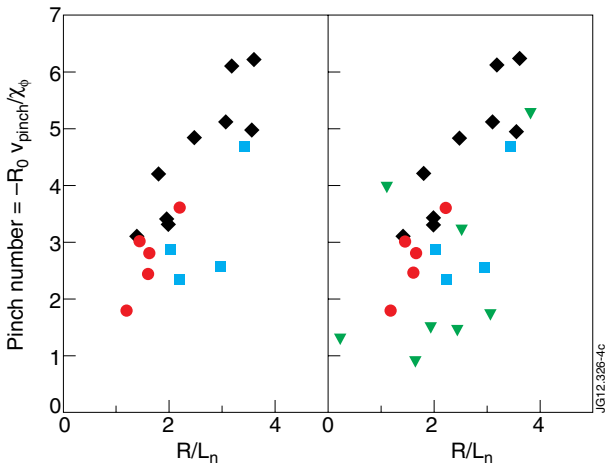

Figure 5: (Left frame) Pinch number as a function of R/L_n from JET (black diamonds), DIII-D (blue squares) AUG (red circles) from the NBI modulation shots. The data have been averaged between $0.4<\rho_{tor}<0.8$. Right frame, as in left frame, but including data from NSTX (green squares) pulses with RMP coil perturbation length R/L_n for JET (black diamonds), DIII-D (blue squares) and AUG (red circles).

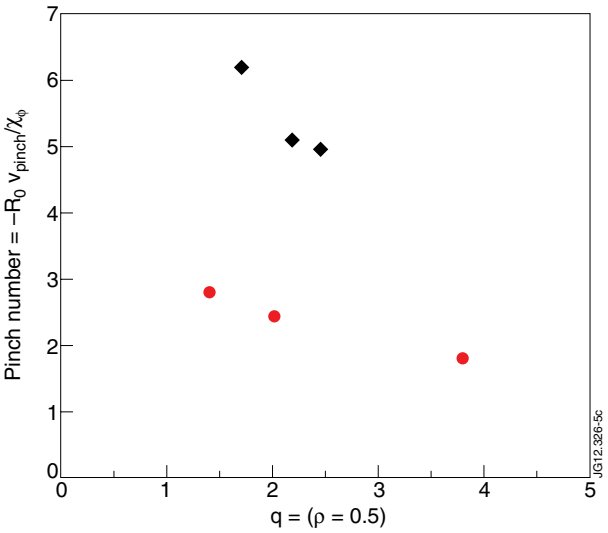

Figure 6: The experimental momentum pinch numbers $-Rv_{pinch}\chi_\phi$ as a function of q value at mid-radius $\rho = 0.5$ from the 3-point q scan from JET (black diamonds) and AUG (red circles) averaged over $0.4<\rho_{tor}<0.8$.